

國立交通大學

電信工程研究所

碩士論文

第四代行動通訊階層式基地台於時間維度  
合作以降低干擾技術之研究

Time Domain Intercell Coordination for  
LTE Hierarchical Cellular Systems

研究生：賴文彬

指導教授：王蒞君 博士

中華民國 一 百 零 一 年 八 月

第四代行動通訊階層式基地台於時間維度合作以降低干擾技術之研究  
Time Domain Intercell Coordination  
for LTE Hierarchical Cellular Systems

研究生：賴文彬

Student : Wen-Pin Lai

指導教授：王蒞君

Advisor : Li-Chun Wang



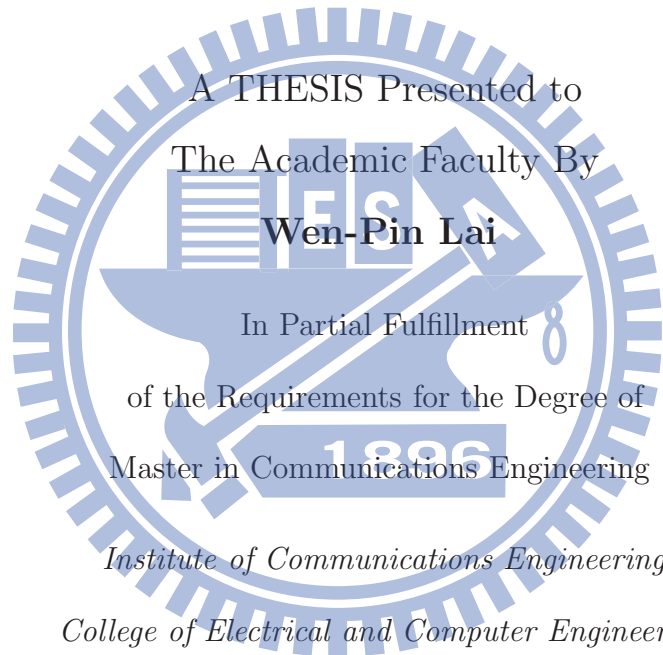
Communications Engineering

August 2012

Hsinchu, Taiwan, Republic of China

中華民國一百零一年八月

**Time Domain Coordination for Intercell  
Interference Reduction in LTE Hierarchical  
Cellular Systems**



A THESIS Presented to  
The Academic Faculty By  
**Wen-Pin Lai**

In Partial Fulfillment  
of the Requirements for the Degree of  
Master in Communications Engineering

*Institute of Communications Engineering  
College of Electrical and Computer Engineering  
National Chiao-Tung University*

August, 2012

Copyright ©2012 by Wen-Pin Lai

# 長期演進技術系統階層式細胞之時間維度合作 降低細胞間干擾

學生：賴文彬

指導教授：王蒞君 教授

國立交通大學

電信工程研究所

## 摘要

增強型細胞間干擾消除(Enhanced inter-cell interference Coordination, eICIC)為一種有效降低細胞間干擾的重要方法相同頻帶。由於在異質性網路中，佈建低功率小基地台可以提升原有細胞的覆蓋範圍以及提升總體吞吐量，因此使用者原有大基地台的範圍下積極佈建，但卻導致小基地台使用者遭受來自大基地台的嚴重訊號干擾。在本論文中，我們針對增強型細胞間干擾消除的時間維度的方法來有效降低細胞間的干擾，並且在細胞範圍延伸(Cell Range Expansion, CRE)保護小細胞的範圍，以及空白子片段(Almost Blank Subframe, ABS)的技術使用下，提出一個以干擾為基礎之適應性空白子片段配置(Interference-aware adaptive ABS allocation)來最大化每個子片段的吞吐量總和，並且提升細胞邊緣使用者的吞吐量。模擬結果顯示可以提升小細胞及大細胞邊緣使用者表現 13%以及 7%，本論文所提出的方法可用來有效提升細胞邊緣干擾減低的重要參考方法。

# Abstract

In this thesis, we present an interference-aware slot allocation technique for improve the system performance of the low-power pico-cells and overlaying macro-cells. In the 3rd Generation Partnership Project (3GPP) Long-Term Evolution- Advanced (LTE-A), this kind of interference between pico-cells and its overlaying macro-cell is called the interference in heterogeneous network (HetNet), which will decrease the coverage area of pico-cells and overall system throughput. In the 3GPP LTE-A cellular system, enhanced inter-cell interference coordination (eICIC) technique adopts Almost Blank Subframes (ABS) to control the inter-cell interference between pico-cells and macro-cells. However, because of the fixed ratio ABS design, the current eICIC techniques will degrade the macrocellular performance severely and the improvement of throughput of pico-cells is also limited in a dynamic traffic environment. Thus, we propose an interference-aware slot allocation technique to adjust the ratio of ABS dynamically based on the estimated interference between macro-cells and pico-cells. Furthermore, the proposed interference-aware slot allocation technique distributively designate the blank slots. Our results show that the proposed interference-aware slot allocation technique can improve the throughput for both macro-cells and pico-cells simultaneously. In the considered case, the throughput of pico-cells and macro-cell cell edge users are improved by at least 13% and 7% respectively, compared to the current fixed ratio ABS design approach.

# Acknowledgments

First, I would like to thank my parents, older sister and younger brother, who always give me endless and powerful supports whenever I was in bad situation. Second, I especially appreciate Professor Li-Chun Wang, who had given me many valuable suggestions in my research during these two years. I would not finish this work without his useful guidance and meaningful comments.

In addition, I cordially give my thanks to my laboratory mates, Ang-Hsun, Ssu-Han, Tsung-Chan, Gen-Hen, Chen-Hsiao and junior laboratory mates at Mobile Communications and Cloud Computing Laboratory at the Institute of Communication Engineering in National Chiao-Tung University. Also, Cheng-Yu, Pei-Chen and Chang-Hui who spent their time with me when I were in need and difficulties. Finally, I'd like to thank 'Chung Hwa Rotary Educational Foundation' about offering me scholarship in research live. I will never forget their help forever. Thanks to the assistances and help from everyone who has helped me all the way.

# Contents

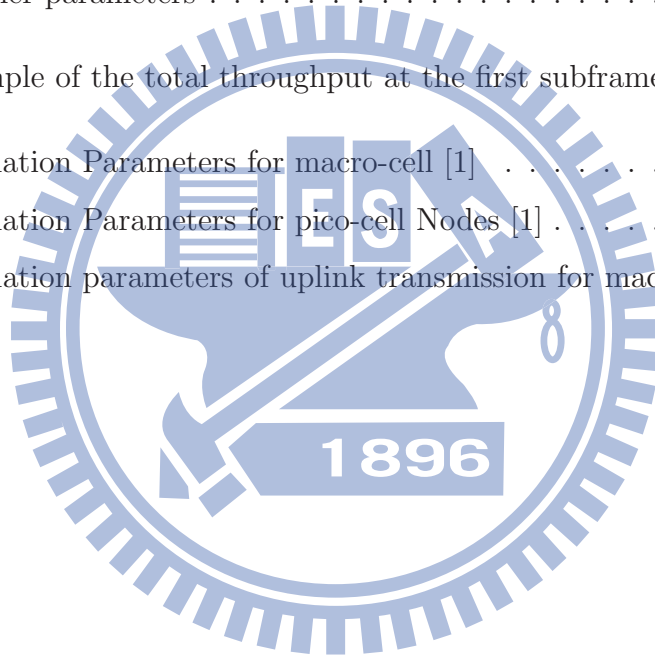
Abstract	i
Acknowledgements	ii
List of Tables	v
List of Figures	vi
<b>1 Introduction</b>	<b>1</b>
1.1 Problem and Solution . . . . .	2
1.2 Thesis Outline . . . . .	3
<b>2 Background</b>	<b>4</b>
2.1 Overview on Heterogeneous Network . . . . .	4
2.2 Introduction to Enhanced Inter-Cell Interference Coordination (eICIC)	5
2.3 Literature Survey . . . . .	8
<b>3 System Models and Problem Formulation</b>	<b>11</b>
3.1 eICIC Baseline Techniques . . . . .	11
3.1.1 Almost Blank Subframe(ABS) . . . . .	11
3.1.2 Centralized and Distributed ABS Allocation Methods . . . . .	15
3.1.3 Cell Range Expansion(CRE) . . . . .	15
3.2 X2 Interface Enhancements for Time-Domain ICIC . . . . .	15
3.2.1 UE side enhancement . . . . .	18

3.3	Doppler Effect . . . . .	21
3.4	Performance Metrics . . . . .	23
3.4.1	System Sum Rate . . . . .	23
3.4.2	Fairness Index . . . . .	23
3.5	Problem Formulation . . . . .	23
<b>4</b>	<b>Interference-aware Adaptive Almost Blank Subframe Allocation in eICIC System</b>	<b>26</b>
4.1	Maximize Throughput of Each Single Subframe . . . . .	26
4.2	Almost Blank Subframe Design . . . . .	28
<b>5</b>	<b>Numerical Results and Discussions</b>	<b>31</b>
5.1	Simulation Assumptions . . . . .	31
5.2	Interference-aware Adaptive ABS Allocation Method . . . . .	34
5.3	Fairness of Our Method and Related Work . . . . .	39
5.4	Prediction of Throughput . . . . .	40
5.5	Uplink Side Transmission . . . . .	40
<b>6</b>	<b>Conclusion</b>	<b>44</b>
6.1	Conclusions . . . . .	44
	<b>Bibliography</b>	<b>45</b>
	<b>Vita</b>	<b>47</b>



## List of Tables

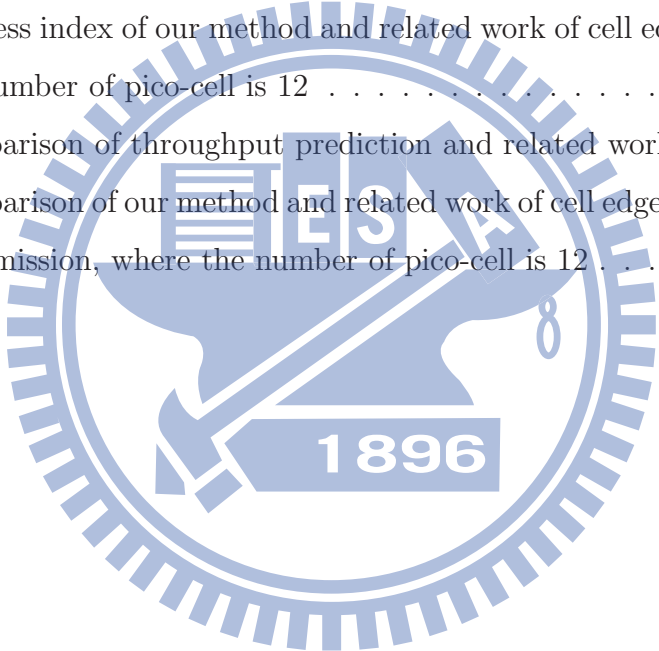
2.1	Literature Survey Summary . . . . .	10
3.1	Key information MIB and SIB carry in LTE . . . . .	20
3.2	Doppler parameters . . . . .	22
4.1	Example of the total throughput at the first subframe with 1 pico-cell	27
5.1	Simulation Parameters for macro-cell [1] . . . . .	32
5.2	Simulation Parameters for pico-cell Nodes [1] . . . . .	32
5.3	Simulation parameters of uplink transmission for macro-cell [1] . . . . .	42

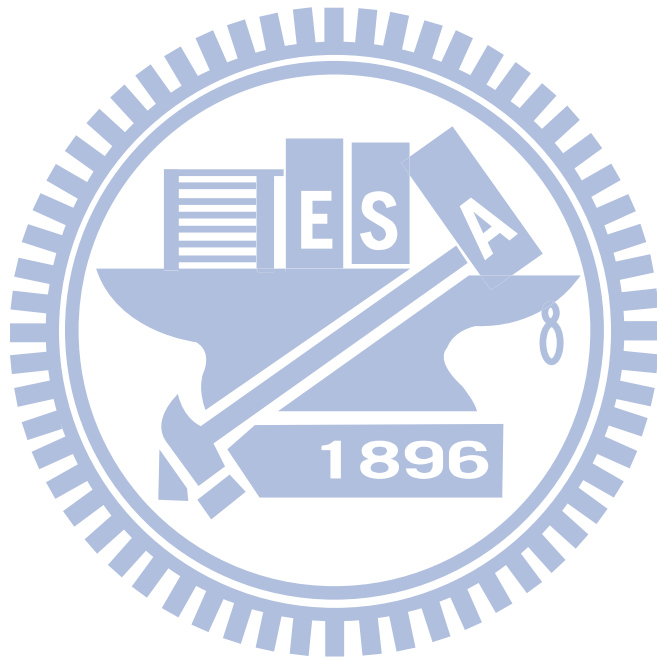


## List of Figures

2.1	Interference Scenarios of eICIC . . . . .	6
2.2	Categorization of the time-domain eICIC solution . . . . .	6
2.3	An example of eICIC based on ABS with subframe alignment . . . . .	7
2.4	An example of eICIC based on lightly-loaded PDCCH with subframe alignment . . . . .	7
2.5	An example of eICIC based on Consecutive subframe blanking with OFDM symbol shift . . . . .	8
3.1	Normal subframe and Almost Blank Subframe . . . . .	12
3.2	Examples of ABS patterns . . . . .	13
3.3	Example of vectors $x_t$ and $y_t$ indicating ABS . . . . .	14
3.4	Cell Range Expansion (CRE) . . . . .	16
3.5	A typical exchange of ABS information over the X2 interface . . . . .	17
3.6	DL Mapping of Logical, Transport and Physical Channels . . . . .	18
3.7	Interference cancellation of acquisition signals and CRS . . . . .	19
3.8	Heterogeneous networks with ABS allocated and CRE adopted in eICIC time domain . . . . .	21
3.9	Downlink radio frame structure . . . . .	22
4.1	Interference-aware adaptive allocated Almost Blank Subframes procedure	29
4.2	Flowchart of Interference-aware adaptive ABS allocation method . . .	30
5.1	Effects of range expansion bias to cell egde users' spectrum efficiency	33

5.2	Comparison of our method and related work of cell edge users, where the number of pico-cell is 6 . . . . .	35
5.3	Comparison of our method and related work of cell edge users, where the number of pico-cell is 12 . . . . .	37
5.4	Comparison of our method and related work of macro-cell cell edge users, where the number of pico-cell is 12 . . . . .	37
5.5	Comparison of mean throughput of our method and related work of cell edge users, where the number of pico-cell is 12 . . . . .	38
5.6	Comparison of our method and related work of cell edge users, where the number of pico-cell is 24 . . . . .	38
5.7	Fairness index of our method and related work of cell edge users, where the number of pico-cell is 12 . . . . .	39
5.8	Comparison of throughput prediction and related work . . . . .	41
5.9	Comparison of our method and related work of cell edge users for uplink transmission, where the number of pico-cell is 12 . . . . .	43





# CHAPTER 1

## Introduction

With the massive growing number of mobile devices and data-intense mobile applications, demands and services in wireless communication has been increasing rapidly in the past few years. It is difficult to get any additional frequency band since the available frequency band is rare now. The low-cost and easy-deployed low power node (LPN), such as RRH, femto-cell, pico-cell and relay node, are consequently deployed to enhance the performance and user throughput within the coverage of macro-cell. With the deployment of small cells mentioned above, we have so called heterogeneous networks, which is one of the representative methods of Long Term Evolution- Advanced (LTE-A) [2]. However, since the operators cannot obtain the exact position of *user-deployed* small cells, strong received power from macro-cell interferes the users of small cells, which not only deteriorates the performance of small cells, but also mitigates the advantages of deploying small cells about offloading the utilization of macro-cell. Hence, enhanced inter-cell interference coordination (eICIC) has been proposed to solve this problem.

There are some researches about resolving the interference between macro-cell and small cells in heterogeneous network with resource partitioning in frequency domain [3] [4]. Resource partitioning in frequency do help mitigate the interference from macro-cell, but still cannot solve the interference when they are in the same frequency. Hence, almost blank subframe (ABS) has been a baseline solution to

eICIC in downlink side [2] [5]. Transmitting only cell-specific reference signal (CRS), PSS and so on in ABS, interference from macro-cell to small cells is consequently mitigated. However, it causes performance and users' throughput loss of the macro-cell side. Hence, in this thesis, we would like to design interference-aware allocated ABS distributed and centralized methods to mitigate the interference from macro-cell side, but maintain the performance of the macro-cell side in heterogeneous network.

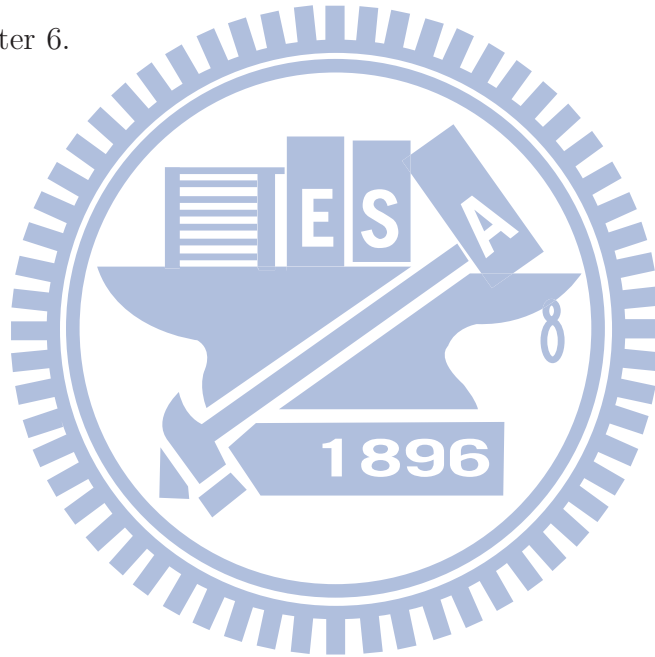
## 1.1 Problem and Solution

In this thesis, we consider a heterogeneous cellular network in which eICIC system is deployed. Since the cell edge users of pico-cells might suffer from severe interference from macro-cell, which not only deteriorate the pico-cell users' throughput, but also decrease the total throughput of entire network. In this situation, eICIC is adopted to enhance the pico-cell users' throughput by allocating almost blank subframes (ABS) to mitigate the interference caused by macro-cell. However, the fixed ABSs can only improve the throughput limitedly since the interference from other pico-cells or macro-cell change dynamically and dramatically. Hence, a interference-aware adaptive allocated Almost Blank Subframes (ABS) design and Cell Range Expansion (CRE) technique in eICIC system are proposed to improve throughput of entire network by finding the optimal ABS allocation. With the above mentioned ABS design, we would like to take advantage of time resource partitioning to assign specific cell to transmit data, and improve the total throughput but still maintain the macro-cell's throughput.

The key contribution of this thesis lies in the design of a interference-aware adaptive allocated Almost Blank Subframes (ABS) method to improve the throughput of interfered cell's users. And also, we provide a solution of the ratio of ABSs over the whole subframes with different number of pico-cells.

## 1.2 Thesis Outline

The rest of this thesis is organized as follows. Chapter 2 introduces the background of heterogeneous and eICIC technique. Some related works are also described and discussed here. Chapter 3 ABS and CRE techniques of eICIC in the heterogeneous network are illustrated first, and then shows the system model and performance metrics also. In Chapter 4, a interference-aware adaptive allocated Almost Blank Subframes (ABS) method is proposed to determine the best Almost Blank Subframes (ABSs) allocation in the next period of time frame time. Then, numerical results and remarks are shown in Chapter 5. Finally, concluding remarks and future works are given in Chapter 6.



# CHAPTER 2

## Background

Neighbor cells are linked by a high-speed backhaul to exchange users' information in the Coordinated Multiple Processing (CoMP) system, and several base stations (BSs) cooperate to provide joint processing of CoMP. However, the higher cost and more complicated architecture design are not favored.

Enhanced inter-cell interference coordination (eICIC) can mitigate ICI between macro-cell and low power nodes (LPNs), such as femto-cell and pico-cell, by resource partitioning in time domain, and also Almost Blank Subframe of eICIC in time domain coordination has been being assumed as a baseline solution in Release 10 [6].

### 2.1 Overview on Heterogeneous Network

As the dramatic growth of traffic demand, cell splitting or additional carriers are widely adopted to overcome throughput and link limitations. In this scenario, all low-cost low power nodes (LPNs), such as pico-cell, femtocell, RRH and relay, are deployed in the same frequency layer to avoid the bandwidth segmentation [7] [8] [9] [10].

Deploying these low-cost BSs enables the flexibility of heterogeneous network. While, the deployment of LPNs results in severe interference. In particular, coverage overlaps between macro cell and LPNs and inter-cell interference is hard to control [11].



There are two kinds of interference scenarios that need to be considered and shown in 2.1 [12] [13]:

1. **Macro-Pico scenario:** In the coverage of Macro cell, users with access to pico-cell are vulnerable to Macro cell's signal interference, and the interference also deteriorates pico-cell users' communication quality (QoS). In particular, pico-cell edge users are severely affected when Cell Range Expansion (CRE) is adopted. Since the transmitting power of pico-cell is not as big as macro-cell's, 30 dBm and 48 dBm, respectively, which is assigned by 3GPP TR 36.814 [1].
2. **Macro-Femto scenario:** When femo-cell belongs to a closed user group (CSG) where access and services are restricted to specific users only. macro-cell users might suffer from severe interference when entering the coverage of femto-cell's.

We mainly discuss the Macro-Pico scenario here in our thesis. In order to suppress the interference in a heterogeneous network and user throughput, Enhanced Inter-Cell Interference Coordination (eICIC) is then introduced in LTE-Advanced (3GPP Release 10) [6] here.

## 2.2 Introduction to Enhanced Inter-Cell Interference Coordination (eICIC)

Different from ICIC, which coordinates only interference on traffic channels in frequency and power control, eICIC can reduce inter-cell interference not only on traffic channels but also on control channels in frequency, time and power domain as well [6].

There are some time-domain eICIC solutions from interference avoidance perspectives have been proposed and categorized in Figure 2.2 [14]:

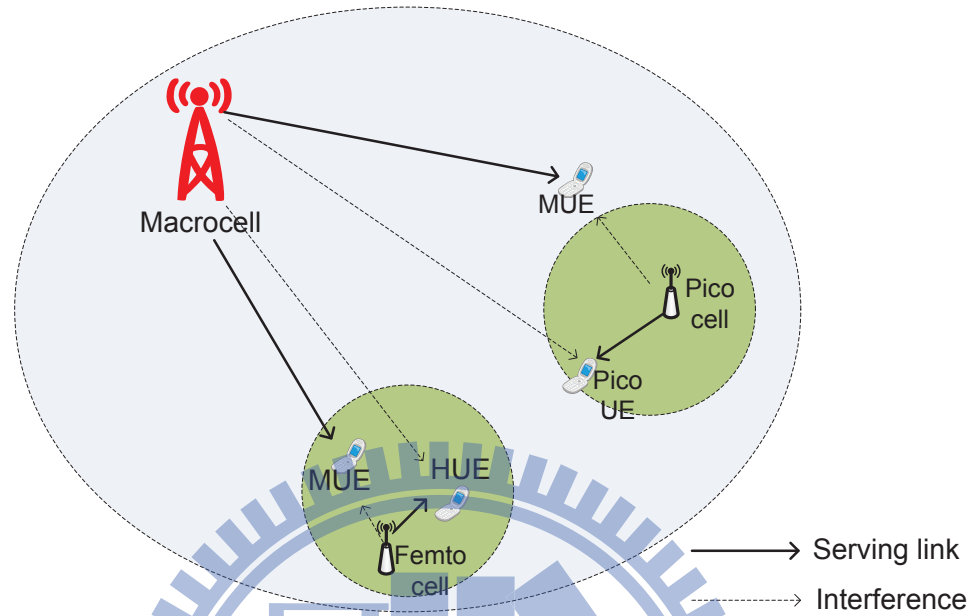


Figure 2.1: Interference Scenarios of eICIC

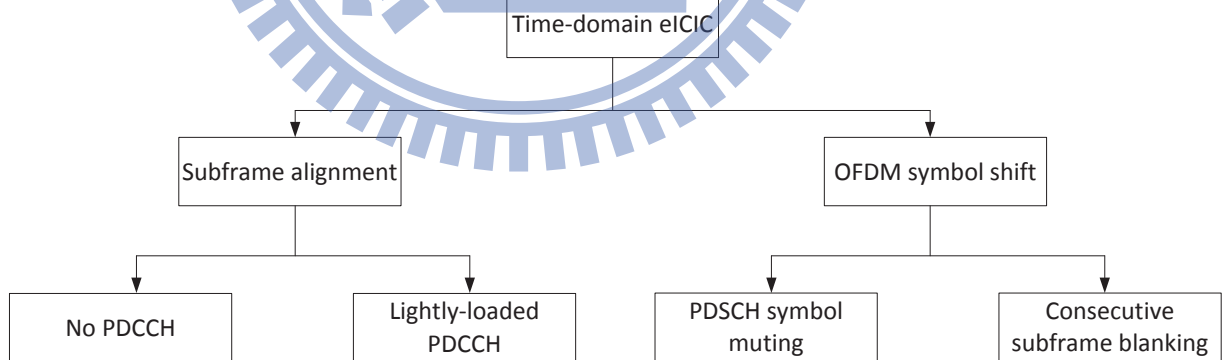


Figure 2.2: Categorization of the time-domain eICIC solution

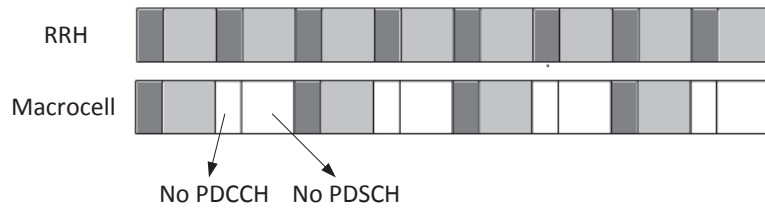


Figure 2.3: An example of eICIC based on ABS with subframe alignment

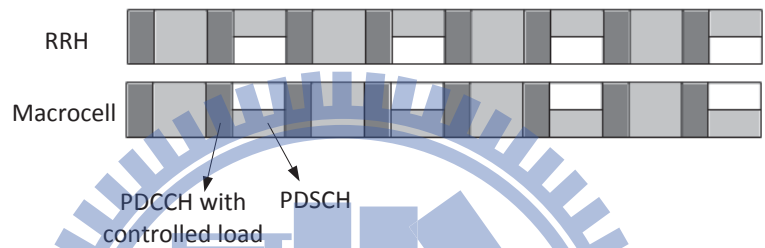


Figure 2.4: An example of eICIC based on lightly-loaded PDCCH with subframe alignment

1. **Subframe alignment:** In this category, the subframe boundary of macro-cell BS and pico-cell BS is aligned. As a result, control and data channels of the macro-cell user will overlap with control and data channels of pico-cell users', respectively. Thus, in order to protect the control channels of the pico-cell users, macro-cell base stations have to coordinate on their PDCCH transmissions. Two different approaches have been proposed in Figure 2.3 and Figure 2.4.
2. **OFDM symbol shift:** In this category, the subframe boundary of pico-cell is shifted by one or more OFDM symbols relatively to that of macro-cell. This symbol-level shift enables the control channel detection of the macro-cell user

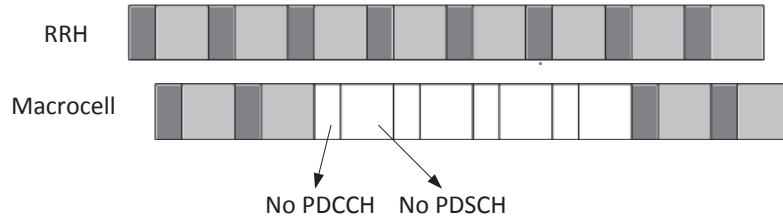


Figure 2.5: An example of eICIC based on Consecutive subframe blanking with OFDM symbol shift

without being interfered by pico-cell's CRS or control channels. On the other hand, the macro-cell user's PDCCH overlaps with pico-cell's PDSCH in this case, so pico-cell has to do some coordination on its PDSCH transmission not to interfere with macro-cell user's control channel detection. Figure 2.5 is one of the examples.

There are also some researches about the interference caused by PDCCH [15] and the impact of extending Rel-8/9 ICIC into Rel-10 [12]. Both of them aim at mitigating interference by coordinating resource in co-channel environment of heterogeneous networks [13].

## 2.3 Literature Survey

[3] provides performance evaluation of the LTE heterogeneous network when small cells are deployed. Cell range expansion and resource partitioning are adopted here. System simulation shows that 4 small cells per macro-cell, 40% or more performance gain can be achieved with FTP traffic model. [4] shows that increasing the number of small cells could increase the mean users' throughput only, but no improvement on total throughput and edge and median users' throughput. While introducing resource partitioning with default strength-based cell selection makes the throughput

unbalance, but could gain additional gain with SINR-based cell selection instead. A trade off between the number of small cells and users' throughput. eICIC in frequency domain can help 5%-tile and 50%-tile user throughputs both improved by 50%. [2] deploys pico-cells and discuss the relationship between bias of CRE and macro cell resource allocation. Almost Blank Subframe (ABS), which only transmits Common Reference Signal (CRS), was adopted here to measure the channel condition and mitigate the interference caused by PDCCH in neighbor cells. CRE can reduce the macro-cell utilization and ABS do help enhance users' throughput. [16] provides a detailed downlink CoMP and eICIC system design in LTE-A heterogeneous network. Results show that the throughput degrades when CoMP is enabled on top of eICIC. eICIC can surely enhance the cell edge users' throughput by adopting time partitioning method with ABS, and also provides a looser coordination method than CoMP. [5] shows that a significant increase of throughput with the deploying of pico-cells, and it also adopts proper CRE bias to solve inter-cell interference issue.

Some researches aim at resource allocation in interference mitigation, [17] provides a radio resource control (RRC) scheme for OFDMA systems where dynamic resource allocation is realized at both a radio network controller (RNC) and base stations (BSs). The adopted scheme is semi-distributed, where RNC makes decision on which channel is used by BS. Here, we take the advantage of semi-distributed method to adaptively allocated ABS based on interference indications. [18] and [19] propose a centralized and distributed resource allocation algorithm to improve the overall throughput. [20] focuses on users throughput maximization and fairness.

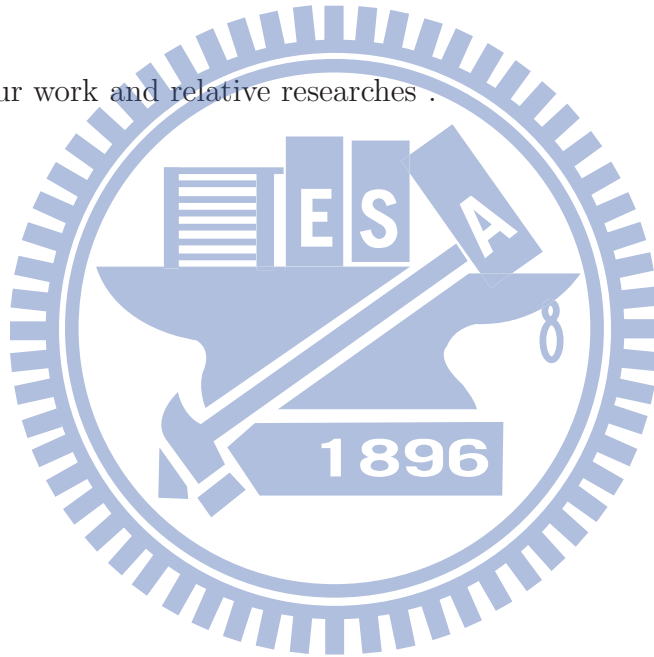
[21] describes the architecture and protocol support for ICIC in the 3GPP system and forms in a flexible way such that operators can employ actual deployment scenario, traffic situation and preferred performance target.

The references mentioned above only prove that eICIC do help mitigate the interference by simulation rather than analysis. Table 2.1 is the literature survey

Table 2.1: Literature Survey Summary

	Partitioning method	Resource allocation	Note
[3]	Frequency	X	
[4]	Frequency	X	
[2]	Time	X	With fixed ABS percentage
[6]	X	V	
Proposed Approach	Time	V	Interference-aware adaptive allocated Almost Blank Subframe

summary of our work and relative researches .



## CHAPTER 3

# System Models and Problem Formulation

### 3.1 eICIC Baseline Techniques

3GPP Release 10 [6] has proposed some baseline techniques to solve the interference problems with eICIC techniques: Almost Blank Subframe (ABS), which mitigates the interference towards the users served by pico-cells in time domain coordination, and Cell Range Expansion or Cell Range Extension (CRE) allows pico-cell users to be served by the cell with weaker power.

#### 3.1.1 Almost Blank Subframe (ABS)

Almost blank subframe (ABS) is the baseline solution that is determined by 3GPP Release 10, and being used in time domain eICIC to mitigate as much as interference towards the victim users as possible. ABS contains some necessary signals with low power, such as synchronization signals (such as SSS and PSS), the physical broadcast channel (PBCH), cell-specific reference signals (CRS) and paging channel (PCH) [22], to reduce the interference to the corresponding subframes of the co-channel victim cell users. A ABS subframe is designed as a normal subframe without redundant signalling, as shown in Figure 3.1.

Figure 3.2 shows three examples of Almost Blank Subframe (ABS) patterns. Figure 3.2(a) shows 1 ABS out of 8 subframes with periodicity of 40 ms, and Fig-

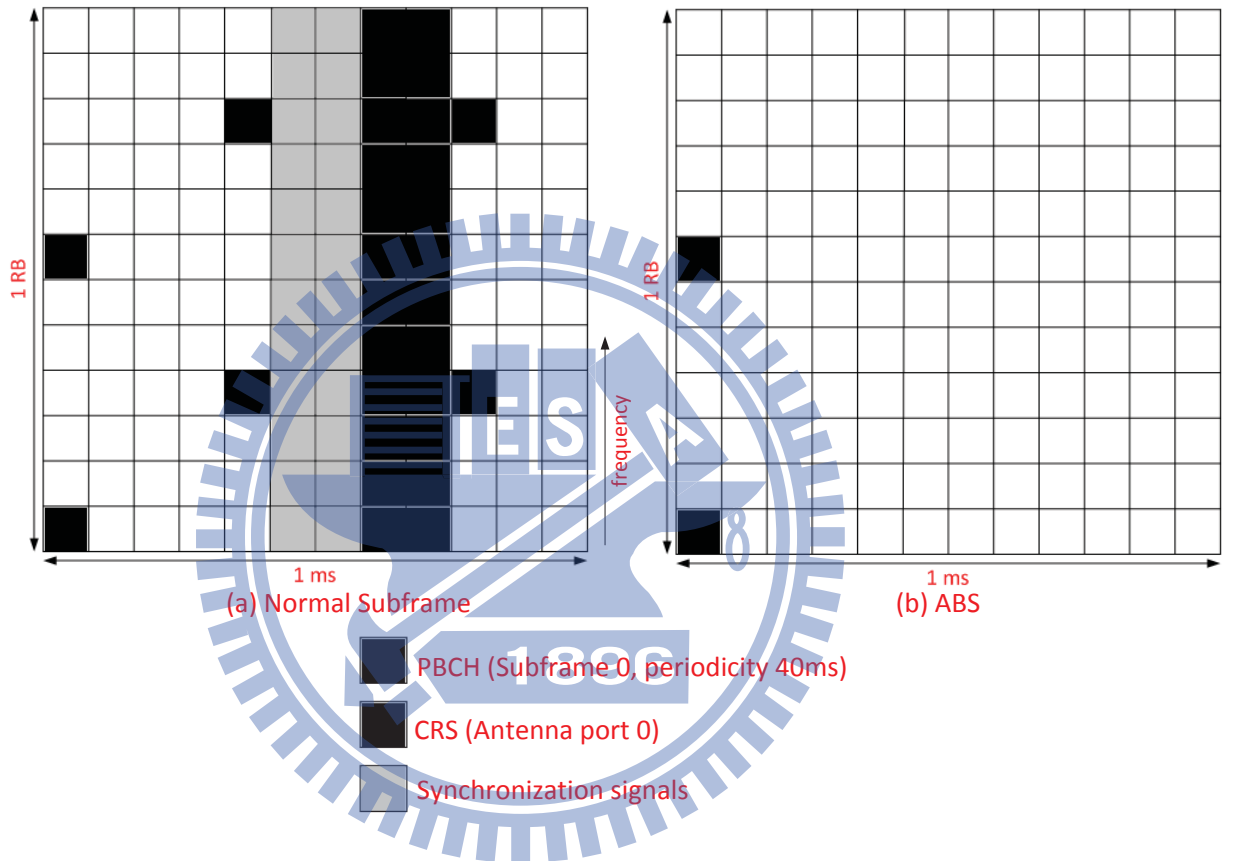


Figure 3.1: Normal subframe and Almost Blank Subframe



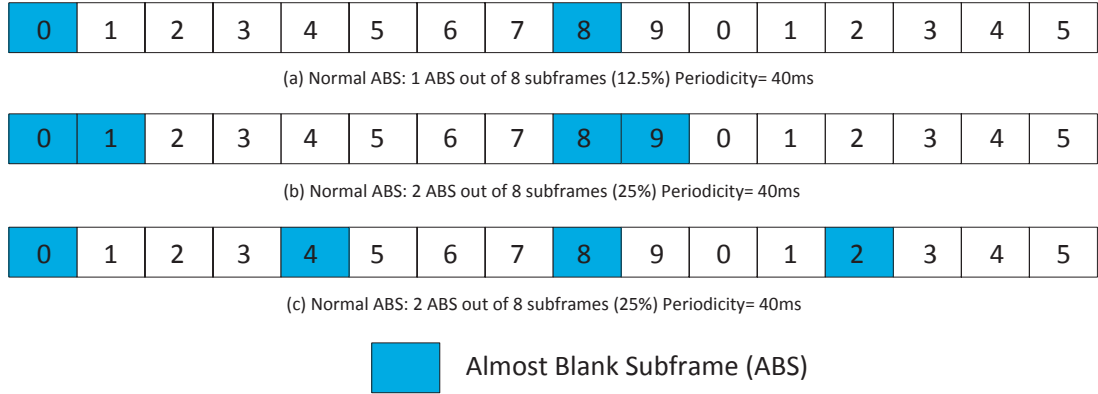


Figure 3.2: Examples of ABS patterns

Figure 3.2(b)(c) illustrate that the different allocation of ABSs from (a) in 40 ms. The more ABSs are allocated in time frames, the higher throughput the victim cell users will gain, but it means that macro-cell might sacrifice its throughput in order to compensate pico-cells'. Hence, it's a trade-off between macro-cell's throughput and pico-cells'.

Besides, in order to allocate of Almost Blank Subframes adaptively, we are going to use vectors  $x_t$  and  $y_t$  to indicate whether macro-cell and pico-cell is allowed to transmit data or not in the  $t$ -th subframe. Indication 1 means that the cell is allowed to transmit in the specific subframe, and 0 otherwise. Here is an example of one of the ABS patterns, which is illustrated in Figure 3.3.

From Figure 3.3, we determine the ratio of ABS over the subframes in a period. A parameter  $R$  is needed here. For example, the parameter  $R$  in Figure 3.3 is:  $R = \frac{\text{sum}(X)}{\text{sum}(Y)} = \frac{1}{8} = 12.5\%$ .

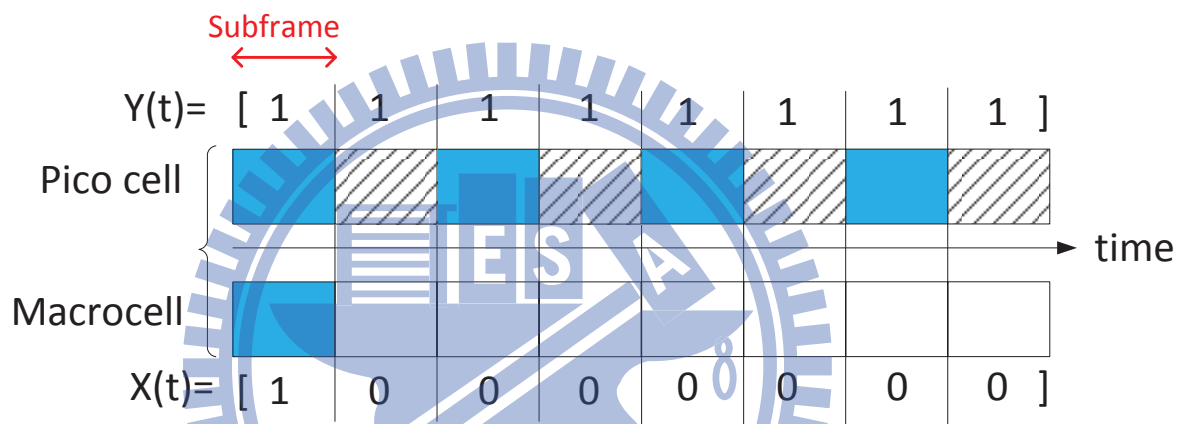


Figure 3.3: Example of vectors  $x_t$  and  $y_t$  indicating ABS

### 3.1.2 Centralized and Distributed ABS Allocation Methods

Each time subframe of ABSs which are suffered from different interference from macro-cell might vary from time to time. According to Figure 3.3, 3GPP and related work blank subframes with centralized method with fixed ABS percentage, while we develop distributed ABS allocation method to allocate blanked subframes based on interference index mentioned above, which mitigate the main interference from macro-cell. In our paper, we will also compare results of our distributed and centralized methods.

### 3.1.3 Cell Range Expansion(CRE)

CRE stands for cell range expansion or cell range extension [23]. If users choose their serving cell by received power or SINR might result in massive loading to macro-cell. Hence the CRE regulates a specific bias to maintain its coverage. In this coverage, CRE allows a user to be served by a cell with weaker received power by biasing a measured power level. And CRE scheme is illustrated in Figure 3.4.

## 3.2 X2 Interface Enhancements for Time-Domain ICIC

Figure 3.5 shows a typical message exchange over the X2 interface for ABS coordination between a macro-cell Base station (BS) and a pico-cell. First, pico-cell invokes function of requesting macro-cell to configure ABS technique. Pico-cell which has been informed about configured ABSs can return an 'ABS Status' message to macro-cell BS that configured the ABSs. This message assists the macro-cell BS in determining whether the percentage of configured ABS should need to be increased

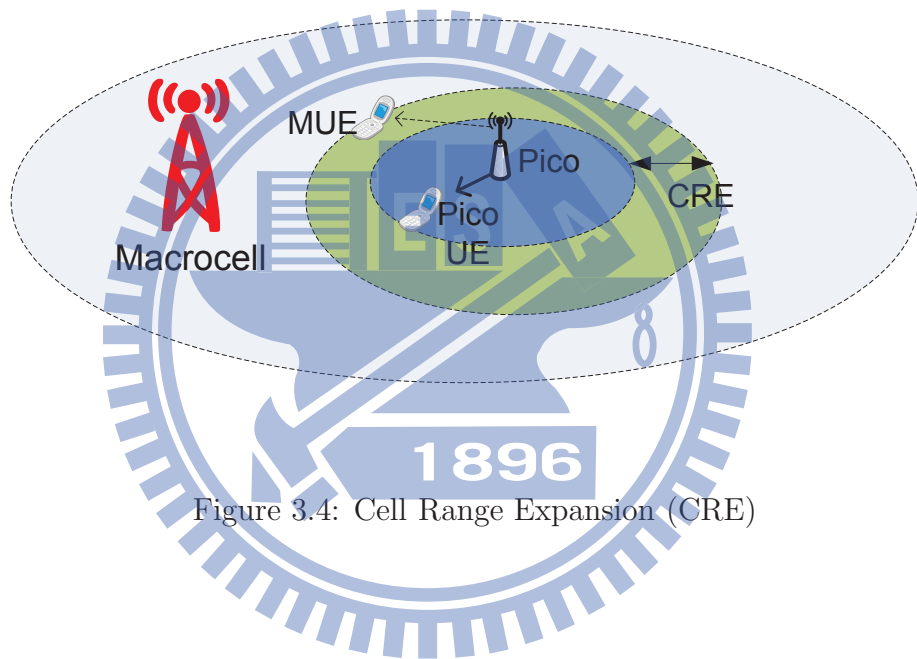


Figure 3.4: Cell Range Expansion (CRE)

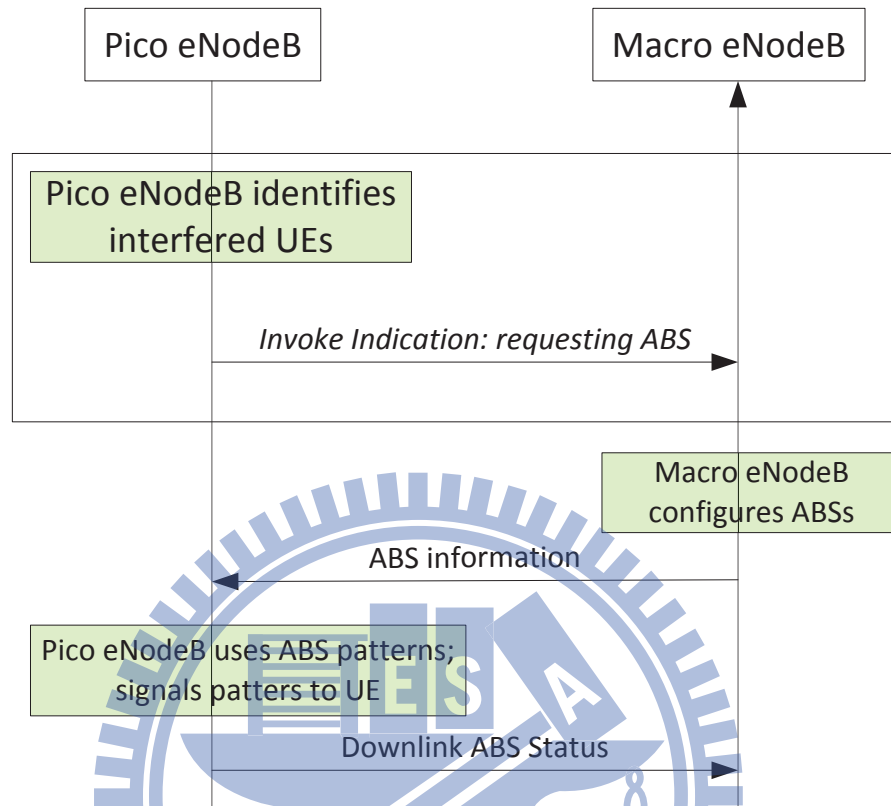


Figure 3.5: A typical exchange of ABS information over the X2 interface

or decreased. Our design put the emphasis on the configures of macro-cell side about how to determine the ratio of all subframes over ABSs.

After obtaining the suitable ratio, which means the percentage of ABS, with different number of pico-cells, then allocate ABSs adaptively according to the interference caused by others.

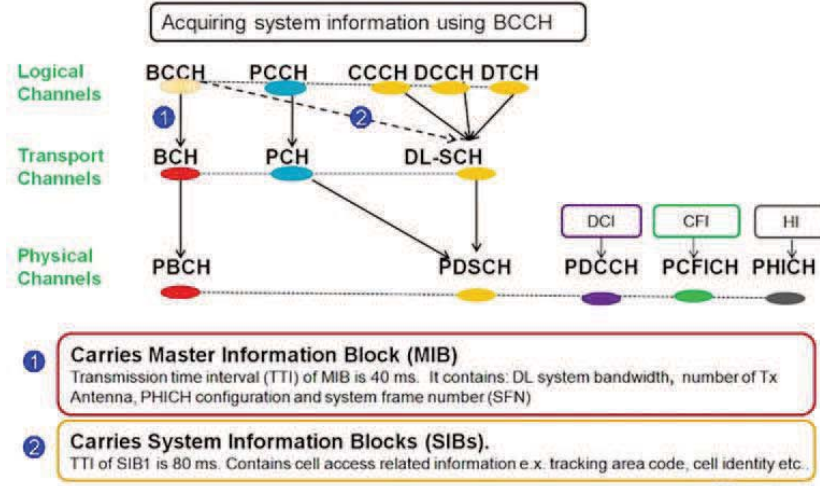


Figure 3.6: DL Mapping of Logical, Transport and Physical Channels

### 3.2.1 UE side enhancement

In our thesis, we assume Macro cell and pico-cells transmit in the same frequency band. The interference detection and cancellation of acquisition signals and cell-specific reference signal (CRS) are important for both macro and pico users. Here, master information block (MIB) and system information block (SIB) are used to distinguish the signal from macro-cell or pico-cell, which has been used in LTE. MIB is transmitted through broadcast channel (BCH), and SIB is transmitted through DL-SCH, which is illustrated in Figure 3.6. The key information MIB and SIB carry is presented in Table 3.2.1. With MIB and SIB, users can distinguish different cell ID from the receiving signal. Then interference detection and cancellation is processed, which is illustrated in Figure 3.7. With the above processes, we can assume that users can detect signal and remove the interference perfectly.

The heterogeneous networks with ABS allocated and CRE adopted in eICIC time domain is illustrated in Figure 3.8. Under the coverage of macro-cell and pico-

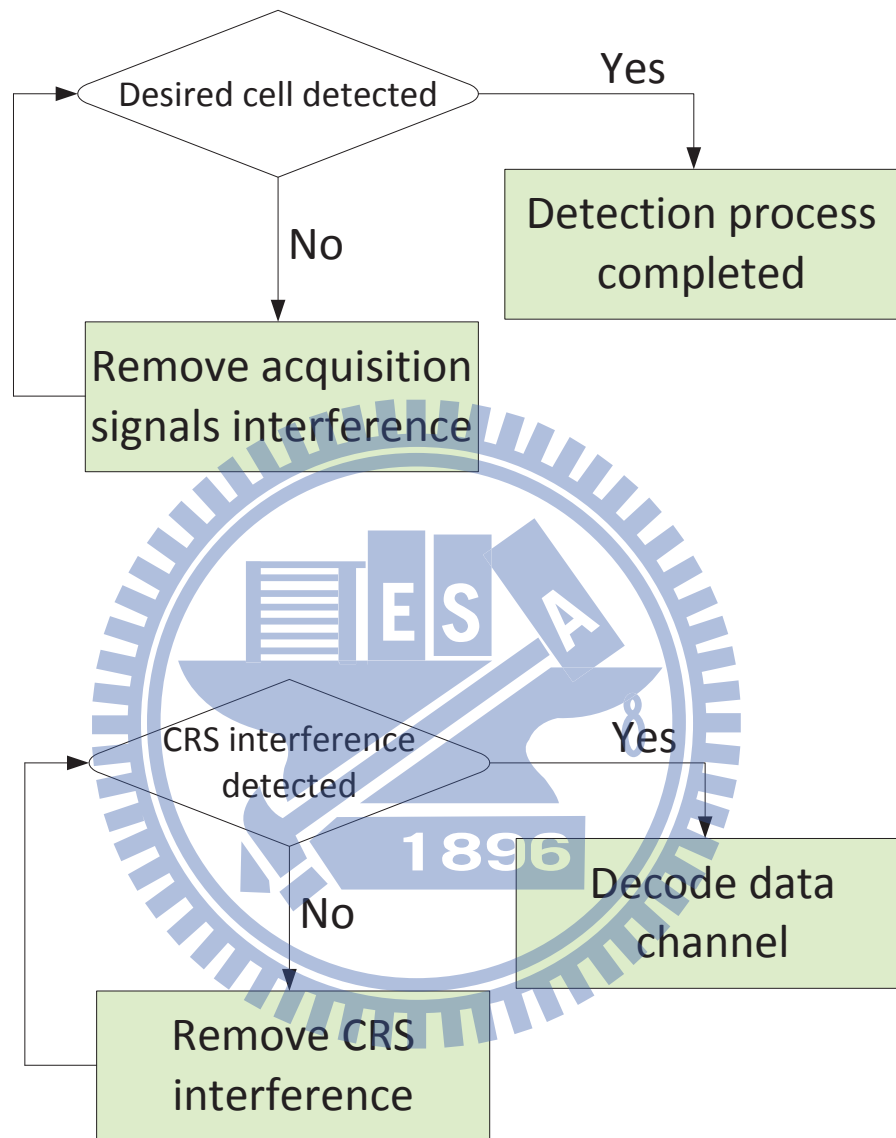


Figure 3.7: Interference cancellation of acquisition signals and CRS

Table 3.1: Key information MIB and SIB carry in LTE

Information Block Type	Key Information
MIB	Downlink bandwidth PHICH configuration System frame number Number of Tx antenna
SIB 1	SIB scheduling list PLMN ID (s) TAC Cell barring Cell selection parameters Frequency band
SIB 2	Detailed cell barring Uplink frequency allocation Uplink bandwidth MBSFN details
SIB 3	Cell re-selection details

cells are deployed inside in the same frequency band, which is the so called co-channel problem. In our thesis, we utilize time resource partitioning to mitigate the interference from macro-cell to the small cells' (pico-cells') users. However, if we sacrifice the performance of macro-cell to compensate pico-cell users' throughput, which might result in huge throughput loss of macro-cell users. As shown in Figure 3.8, macro-cell user and pico-cell user can transmit in the colored subframes while macro-cell cannot transmit data in white subframes, which are the ABSs. Figure 3.9 shows the structure of one radio frame, which contains 20 time slots with 0.5 ms of each. In order to align



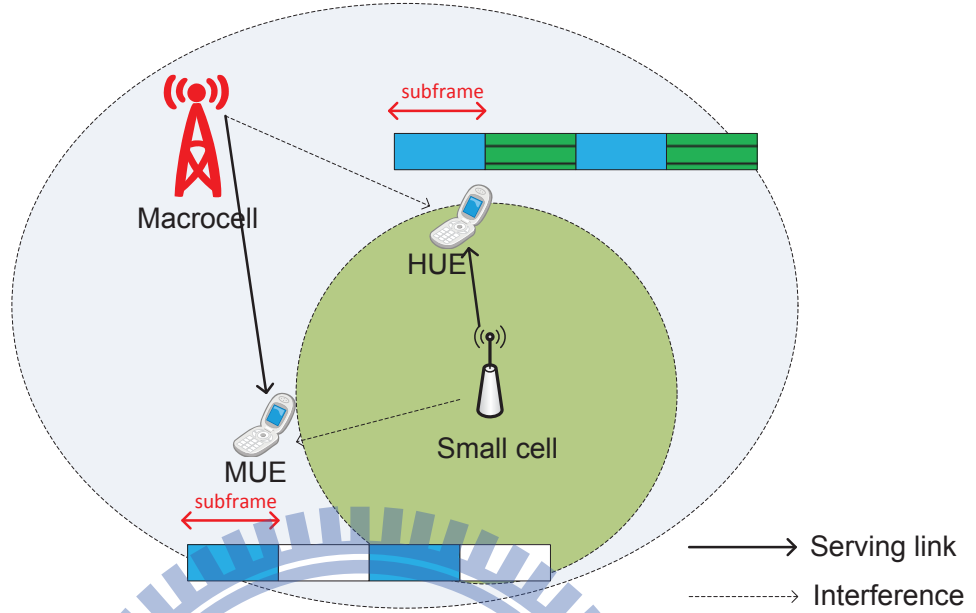


Figure 3.8: Heterogeneous networks with ABS allocated and CRE adopted in eICIC time domain

with the uplink round trip time [6], the periodicity for time domain configuration of ABS is also 20 ms.

### 3.3 Doppler Effect

From the point of view of the mobile users, we need to take time and frequency coherence into consideration. Hence Doppler frequency is given by:

$$f_d = f_c \left( \frac{v}{c} \right) \cos \alpha_n \quad (3.1)$$

where  $f_c$  is the carrier frequency,  $v$  is the speed of mobile user,  $c$  is the speed of light and  $\cos \alpha_n$  is the incident angle. Table 3.2 shows the parameters of Doppler effect.

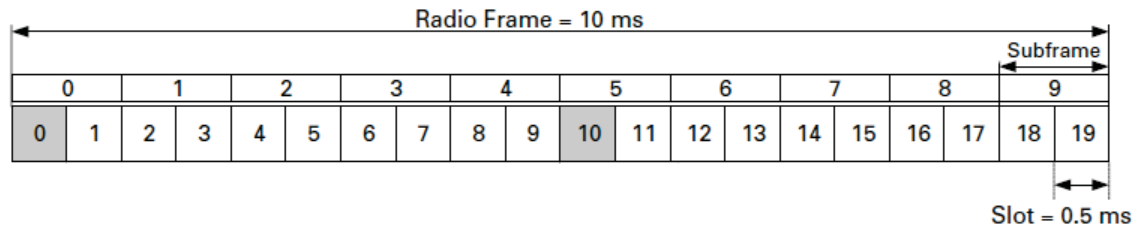


Figure 3.9: Downlink radio frame structure

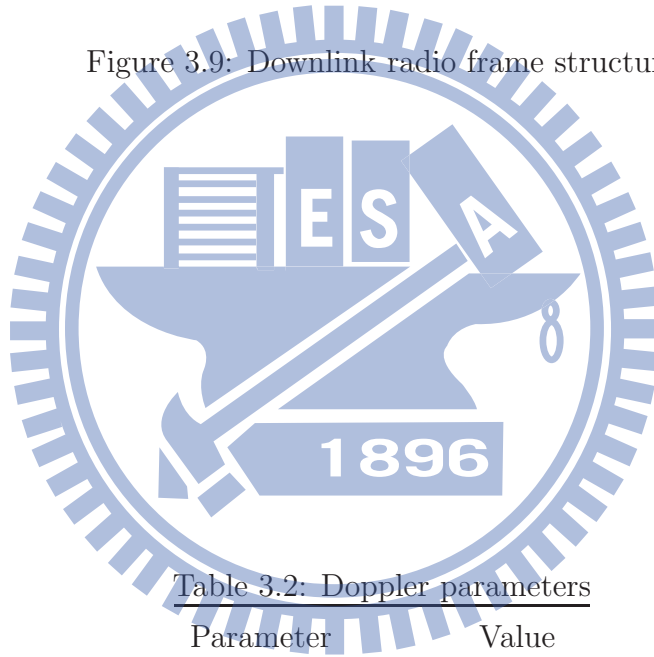


Table 3.2: Doppler parameters

Parameter	Value
User Speed	3 km/hr
Frequency carrier	2G Hz

## 3.4 Performance Metrics

### 3.4.1 System Sum Rate

We consider a multi-user broadcast system, and utilize Shannon capacity formula to model the system sum rate as follows:

$$C_{sum} = \sum_U \log_2(1 + \gamma_u) \quad (3.2)$$

where  $U$  is the set of served users in the entire network;  $\gamma_u$  is the signal to interference and noise ratio (SINR) of the  $u^{th}$  user.

### 3.4.2 Fairness Index

Fairness is used to determined whether all the users share the resource fairly. In this thesis, we use Jain's Fairness Index as follows:

$$F(x_1, \dots, x_k) = \frac{\left(\frac{1}{K} \sum_{i=1}^k x_i\right)^2}{\frac{1}{K} \sum_{i=1}^k x_i^2} = \frac{\left(\sum_{i=1}^k x_i\right)^2}{K \sum_{i=1}^k x_i^2} \quad (3.3)$$

where  $x_i$  is the number of resource allocating to the  $i^{th}$  user;  $K$  is the number of users. The larger the fairness the index  $F$  is, the more the fair the resource allocate. The range of  $F$  is between  $\frac{1}{K}$  and 1, where  $\frac{1}{K}$  represents the worst case with all resources are allocated to one user. If fairness is equal to one, it represents that all users are allocated the same amount of resource.

## 3.5 Problem Formulation

Based on the system model in Section3.1.1 and 3.1.3, We consider an OFDMA system in a specific bandwidth channel, and a network of  $L$  cells. Let  $\mu_l$  be the user set for

macro-cell.  $R_l$  denotes Pico in  $L$ -th cell. And

$$R_l = \sum_{i=1}^N R_{l_i} \quad (3.4)$$

where  $N$  is the number of pico-cell.

Hence, the entire network has a total users of  $U_{total}$  which is:

$$U_{total} = \sum_{l=1}^L (M_l + R_l) \quad (3.5)$$

And assume the achievable throughput(bps) is determined by SINR:

$$Capacity = \log_2\left(1 + \frac{Signal}{Interference + Noise}\right)(bits/s) \quad (3.6)$$

Then, we can assume achievable throughput (bps) of macro-cell users and pico-cell users of with and without interference in a *period t*:

$\mathbf{I}_t^{Macro} = [i_t^{Macro}]_{t \times M_l}$  : macro-cell users achievable throughput (bps) matrices with interference from pico-cell and macro-cell.

$\mathbf{S}_t^{Macro} = [s_t^{Macro}]_{t \times M_l}$  : macro-cell users achievable throughput (bps) matrices without interference from macro-cell.

$\mathbf{I}_t^{Pico} = [i_t^{Pico}]_{t \times R_l}$  : pico-cell users achievable throughput (bps) matrices with interference from pico-cell and macro-cell.

$\mathbf{S}_t^{Pico} = [s_t^{Pico}]_{t \times R_l}$  : pico-cell users achievable throughput (bps) matrices without interference from macro-cell.

Note:  $\mathbf{I}$  and  $\mathbf{S}$  are throughput matrices at time period  $t$  for macro-cell or pico-cell

$$\mathbf{I}_t = \log_2\left(1 + \frac{Signal}{\underbrace{Interference + Noise}_{Macro \text{ and Pico}}}\right), \quad (3.7)$$

$$\mathbf{S}_t = \log_2\left(1 + \frac{\text{Signal}}{\underbrace{\text{Interference} + \text{Noise}}_{\text{Macro or Pico}}}\right). \quad (3.8)$$

With the aforementioned definitions, we maximize each subframe by the interference and by designing the allocation of ABSs which could be assigned by vector  $x_t$ .



## CHAPTER 4

# Interference-aware Adaptive Almost Blank Subframe Allocation in eICIC System

### 4.1 Maximize Throughput of Each Single Subframe

With the previous definitions, in order to improve the pico-cell edge user's throughput who suffered from huge interference from macro-cells. We obtain total throughput of each subframe from pico-cell side and macro-cell side. Hence, we could evaluate and design how to allocate the ABS in the next period.

First,  $y_t$  is the indicating vector of pico-cell with ABS, and  $x_t$  represents the indicating vector of macro-cell. Hence, we can get the total throughput (bps) of  $N$  pico-cells:

$$N( \underbrace{y_{1 \times t} I_{t \times R_l}^{Pico}}_{\text{Achievable transmission rate of a pico-cell}} - \underbrace{x_{1 \times t} (S_{t \times R_l}^{Pico} - I_{t \times R_l}^{Pico})}_{\text{Interference from macro-cell}} ) \quad (4.1)$$

From (4.1), the first term is the total throughput of a pico-cell without macro-cell's interference, while the second term is the interference from macro-cell.

Here is a simple example of equation (4.1) with  $N=1$  and at  $t=1$ , which means the total throughput (bps) at the first subframe with *one* pico-cell.

Table 4.1: Example of the total throughput at the first subframe with 1 pico-cell

$t=1$	$N(y_{1 \times t} I_{t \times R_l}^{Pico} - x_{1 \times t} (S_{t \times R_l}^{Pico} - I_{t \times R_l}^{Pico}))$
$x_1=1, y_1=1$	$2I_{1 \times R_l}^{Pico}$
$x_1=0, y_1=1$	$I_{1 \times R_l}^{Pico}$

Different from the pico-cell side, the total throughput of macro-cell is relatively simple. In our scenario, we assume users of pico-cells can transmit data at every subframe, and macro-cell can arrange its users transmission in specific subframes only. Consequently, we formulate the total throughput of macro-cell's as:

$$x_{1 \times t} S_{t \times M_l}^{Macro} - y_{1 \times t} (S_{t \times M_l}^{Macro} - I_{t \times M_l}^{Macro}) \quad (4.2)$$

In order to obtain the total throughput of *all users* in each subframe. We sum up the achievable throughput of both sides from (4.1) and (4.2):

$$\begin{aligned} & \sum_{R_l=1}^{R_l} N(y_{1 \times t} I_{t \times R_l}^{Pico} - x_{1 \times t} (S_{t \times R_l}^{Pico} - I_{t \times R_l}^{Pico})) \\ & + \sum_{M_l=1}^{M_l} x_{1 \times t} S_{t \times M_l}^{Macro} - y_{1 \times t} (S_{t \times M_l}^{Macro} - I_{t \times M_l}^{Macro}) \end{aligned} \quad (4.3)$$

Then from the first term of (4.3) can be illustrated as:

$$\begin{bmatrix} 1 & 0 & \cdots & 0 & 1 \end{bmatrix}_{1 \times t} \begin{bmatrix} A_{11} & A_{12} & \cdots & A_{1R_l} \\ A_{21} & A_{22} & \cdots & \vdots \\ \vdots & \vdots & \ddots & \vdots \\ A_{t1} & A_{t2} & \cdots & A_{tR_l} \end{bmatrix}_{t \times R_l} = [B]_{1 \times R_l} \quad (4.4)$$

and the dimension of the second term is:

$$\begin{bmatrix} 1 & 0 & \cdots & 0 & 1 \end{bmatrix}_{1 \times t} \begin{bmatrix} C_{11} & C_{12} & \cdots & C_{1R_l} \\ C_{21} & C_{22} & \cdots & \vdots \\ \vdots & \vdots & \ddots & \vdots \\ C_{t1} & C_{t2} & \cdots & C_{tR_l} \end{bmatrix}_{t \times M_l} = [D]_{1 \times M_l} \quad (4.5)$$

Finally, we combine (4.4) and (4.5) into one matrix, and get:

$$Z_t = \left[ \begin{array}{c|c} B & D \end{array} \right]_{1 \times (M_t + R_t)} \quad (4.6)$$

where (4.6) represents the total throughput (bps) of all users in a period of time, and then maximize  $z_t$  by designing  $x_{1 \times t}$ .

## 4.2 Almost Blank Subframe Design

Fixed position of time frames will cause unnecessary throughput loss. While, in our design, we propose an adaptively assigned ABS time subframes according to interference index  $\mathbf{K}$ .

From equation (4.6), we determine  $x_{1 \times t}$  vector according to  $I_{t \times R_t}^{Pico}$ ,  $S_{t \times R_t}^{Pico}$  and  $I_{t \times M_t}^{Macro}$  to allocate subframes in the next time period from with achievable throughput (bps) with and without interference. Figure 4.1 illustrates the procedure of the proposed allocation method.

First, we find the matrices  $\mathbf{I}$ ,  $\mathbf{S}$  and  $\mathbf{K}$ . Arrange  $\mathbf{K}$  in decreasing order, blank the frame with large  $\mathbf{K}$  and get  $z'_t$ . To compare with original ABS pattern with value  $z_t$ , we choose the large one of  $z'_t$  and  $z_t$ . This algorithm repeats every time period with 20 ms.

With the procedure and the indication of  $x_{1 \times t}$ , the flowchart shows how the algorithm goes to reallocate the ABS allocation adaptively according to the interference, which is shown in Figure 4.2. Algorithm starts from environment setup and generates the ABS percentage, and apply interference-aware allocated ABS method to allocate ABSs adaptively.



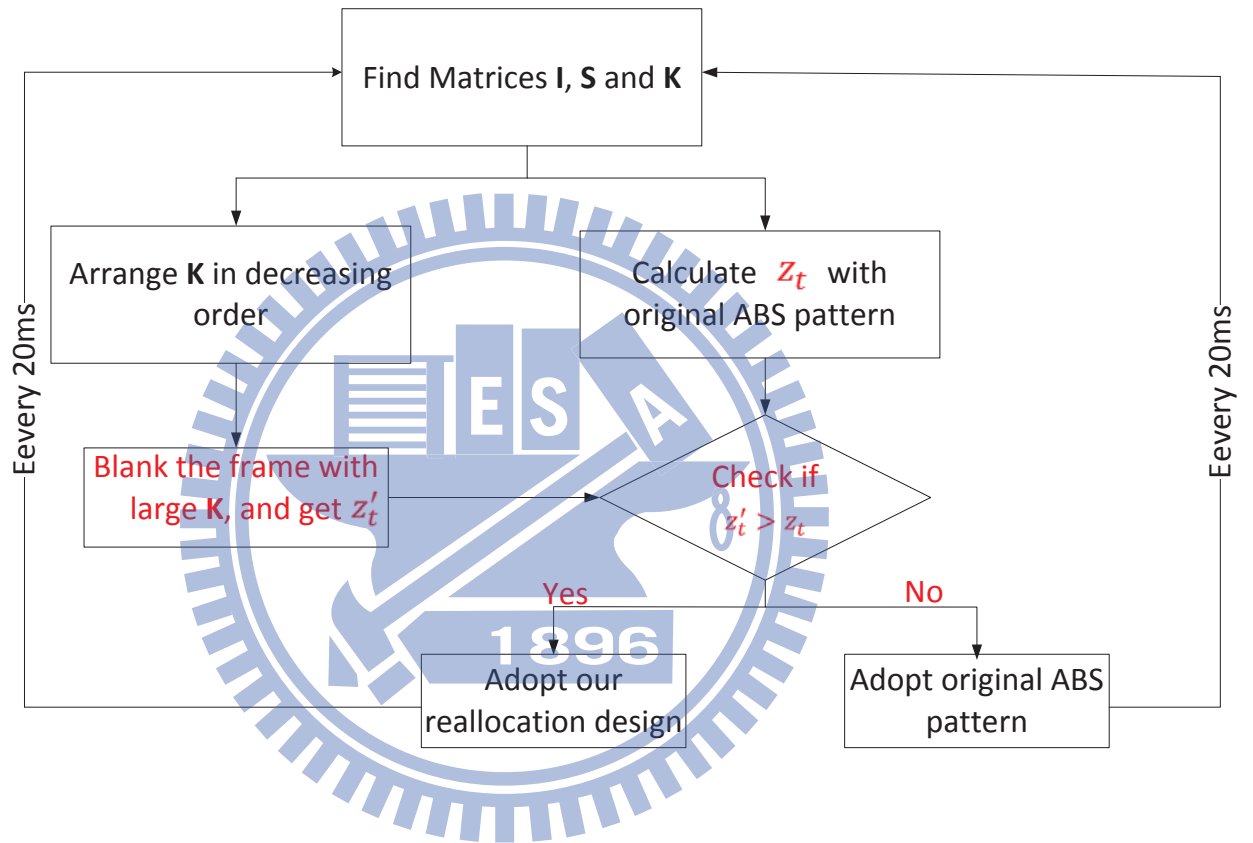


Figure 4.1: Interference-aware adaptive allocated Almost Blank Subframes procedure

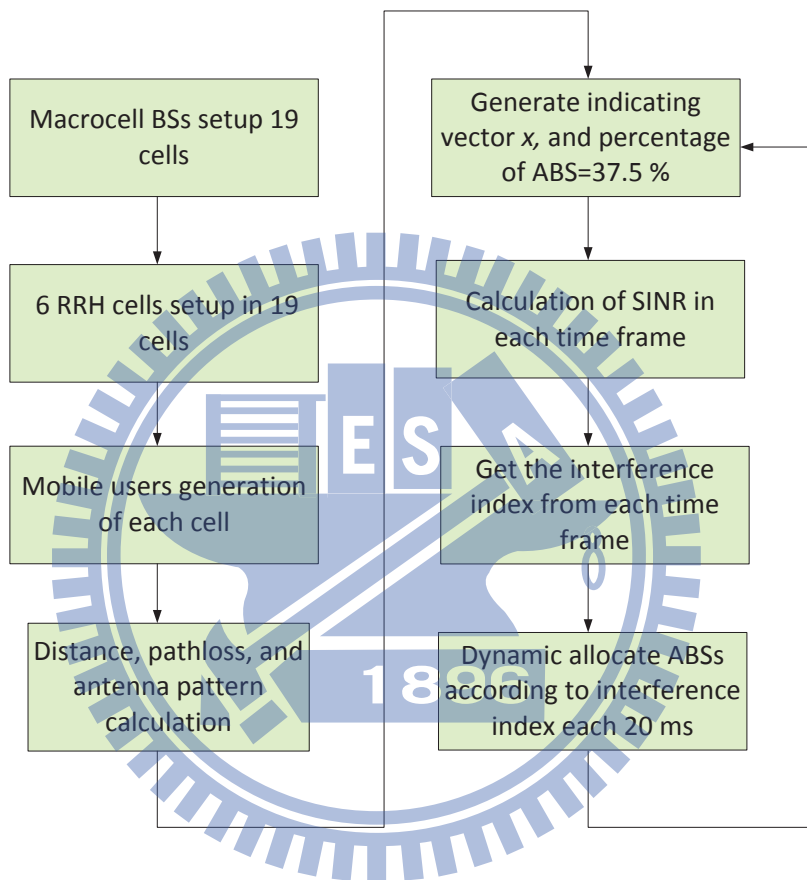


Figure 4.2: Flowchart of Interference-aware adaptive ABS allocation method

## CHAPTER 5

# Numerical Results and Discussions

### 5.1 Simulation Assumptions

In this section, we describe the simulation environments for evaluating the performance of the proposed interference-aware adaptively ABS allocation method. The simulation setup follows the assumptions given in the 3GPP evaluation methodology specification for LTE-Advanced [1], where the bandwidth is 10 MHz; penetration loss is 20 dB. And the distribution of all 19 cells are located with a macro-cell and pico-cells and their users. The users of macro-cell and pico-cell are located randomly. We allocate 300 users in macro-cell coverage and 50 users for each pico-cell coverage according to the area of them. The radius of each cell is 500 meters. The transmit power of macro-cell and pico-cell is 46 dBm and 30 dBm, respectively. The noise power density is -174 dBm. All simulation parameters are listed in Table 5.1 and Table 5.2, which is for macro-cell and pico-cell respectively.

First, we would like to know the effects of cell range bias to cell edge users. Figure 5.1 shows that the larger bias might offload traffic from macro-cell, but deteriorate pico cells' throughput. Hence, it is preferable to choose on the order of 8 dB.

Table 5.1: Simulation Parameters for macro-cell [1]

Parameter	Value
Link Direction	Downlink
Bandwidth	10 MHz
Macro-cell layout	19 Base Stations
Inter-site distance	500 meters
Penetration Loss	Macro: $128.1+37.6*\log_{10}(d)$ , d in km
Antenna Pattern	$A_H(\phi) = -\min\left[12\left(\frac{\phi}{\phi_{3dB}}\right), A_m\right]$ , $\phi_{3dB} = 70^\circ$ , $A_m = 25dB$
Max Tx Power	46 dBm
Noise Power Density	-174 dBm/Hz
Shadowing	8 dB
Minimum Distance between User and Macro-cell	35 meters

Table 5.2: Simulation Parameters for pico-cell Nodes [1]

Parameter	Value
Pico-cell layout	Deterministic at a distance of $\frac{3}{4}$ Macro-cell radius from the Macro-cell center
Number of picos per cell	3, 6, 12
Pathloss Model	Pico: $147.7+36.7*\log_{10}(d)$ , d in km
Antenna Pattern	Pico: Omni-antennas
Max Tx Power	30 dBm
User Speed	3 km/hr
Bias of Pico Cell Range	8 dB
Shadowing	10 dB

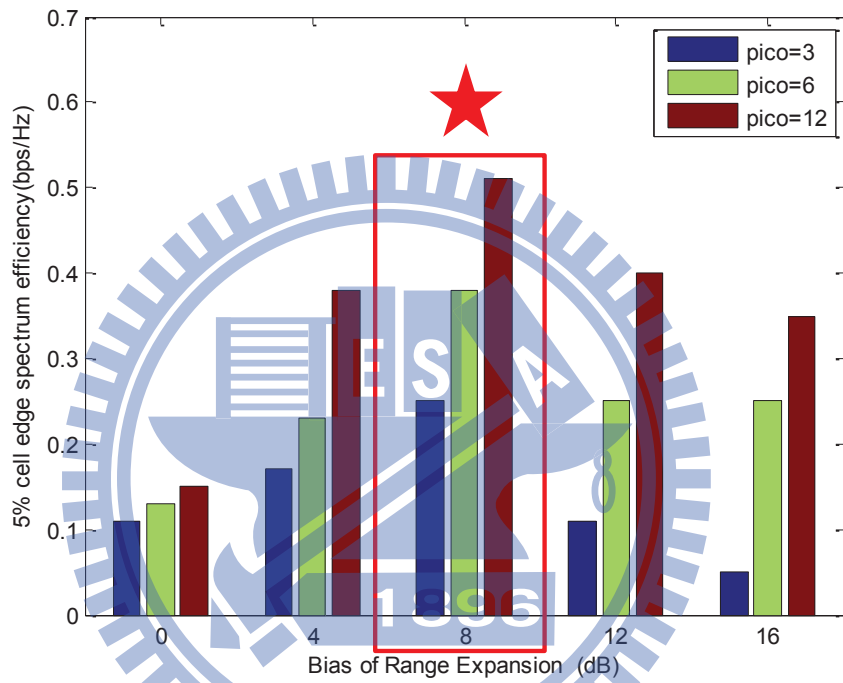


Figure 5.1: Effects of range expansion bias to cell edge users' spectrum efficiency

## 5.2 Interference-aware Adaptive ABS Allocation Method

With the ABS pattern in Figure 3.1 and setup environment mentioned above, we would like to compare our method with [2], which proposes a fixed 50% ABS allocation method and 8 dB cell range expansion bias. Hence, based on several techniques we have considered and simulate centralized and distributed ABSs allocation methods. The following results are as below:

In Figure 5.2, we sketch spectrum efficiency with different percentage of our work with distributed allocation, centralized allocation and related works with 6 pico-cells overlaying in a macro-cell. We can notice that centralized and distributed ABS allocation performs almost the same with 6 pico-cells, which is 0.49 (bps/Hz/user) and 0.48 (bps/Hz/user) for distributed and centralized allocation methods, respectively. It is because that centralized method use the same ABS pattern all the time regardless of interference index, while distributed method can adaptively allocate ABS slots according to interference index mentioned above. Hence, we could find out the importance of time slots allocation according to interference index matrices of each time period, which can mitigate the interference for pico-cell users caused by macro-cells.

It also shows that our distributed or centralized methods perform better than [2] with different ABS percentage. The spectrum efficiency of throughput cell edge users can reach 0.49 (bps/Hz/user) with our method, which gains extra 10% out of related work with 0.44 (bps/Hz/user) at 37.5%, where x-axis is the percentage of ABS and y-axis is the user throughput of macro-cell users and pico-cell users. Since our adaptive ABS method can effectively mitigate the interference from macro-cell by blanking subframes and alleviate pico-cell cell edge users' throughput. While there is a climax at 37.5%, which is the best percentage to achieve highest spectrum efficiency

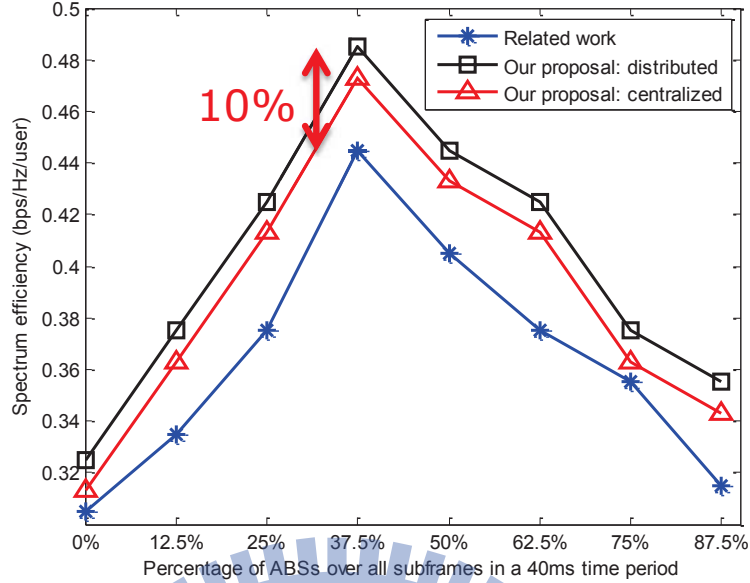


Figure 5.2: Comparison of our method and related work of cell edge users, where the number of pico-cell is 6

with 6 pico-cells. If higher percentage of ABS is adopted here, the lower interference for pico-cell users and the spectrum efficiency of pico-cell users can be alleviated consequently. In the contrary, it sacrifices macro-cell users' throughput, and decrease macro-cell users' spectrum efficiency. Therefore, we need to find out the best ABS percentage, which can reach the highest spectrum efficiency for both macro-cell and pico-cell users.

Figure 5.3 shows that our proposed method improves cell edge users throughput by 15% with 0.77 (bps/Hz/user) and 0.68 (bps/Hz/user) of related work. This figure also sketch two lines about the results of shadowing and Doppler effects. Doppler effect take frequency shift into consideration and improves additional gain to spectrum efficiency. Shadowing can enhance spectrum efficiency by around 7% and Doppler can increase by additional 3% with spectrum efficiency at different ABS percentage.

In addition, our proposed distributed and centralized methods can also maintain the mean throughput of users when we enhance the spectrum efficiency of cell edge users, which is shown in Figure 5.5, our spectrum efficiency at 37.5% ABS percentage can reach 2.85 (bps/Hz/user) , 2.83 (bps/Hz/user) for centralized and distributed methods. While related work only reaches 2.8 (bps/Hz/user), which is not as good as our methods.

Since the problem about determining the suitable ABS percentage is highly related to the deployment number of pico-cells, we determine when the best number when pico-cells is 12, which is shown in Figure 5.3, the max spectrum efficiency of all users is around 25%, which is lower than 6 pico-cells'. It is because that pico-cells can improve user throughput by deploying more pico-cells, blanking more ABS is not necessary. As for macro-cell users, from Figure 5.4, we can find out that the spectrum efficiency gets worse when ABS percentage is higher. The highest spectrum efficiency locates at 0%, which is different with Figure 5.3, 0.85 (bps/Hz/user). However, according to Figure 5.5, we choose 25% to maximize the spectrum efficiency with 12 pico-cells.

When more pico-cells are deployed, which is 24 pico-cells. Extra 17% improvements is shown in Figure 5.6 as well, where our methods reach 0.83 (bps/Hz/user), 0.79 (bps/Hz/user) for centralized and distributed methods, and 0.7 (bps/Hz/user) of related work at 12.5% ABS percentage. This result can also verify that when more pico-cells are deployed, the lower ABS percentage we need to enhance spectrum efficiency. Moreover, the more pico-cells are deployed, the lower ABS percentage is needed.

We can also conclude from Figure 5.2, Figure 5.3 and Figure 5.6, the more pico-cells are deployed, the higher the spectrum efficiency of cell edge users.



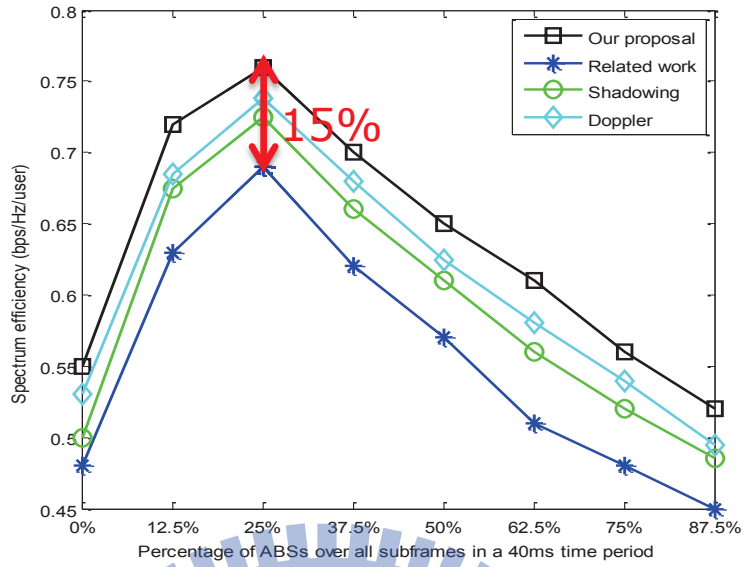


Figure 5.3: Comparison of our method and related work of cell edge users, where the number of pico-cell is 12

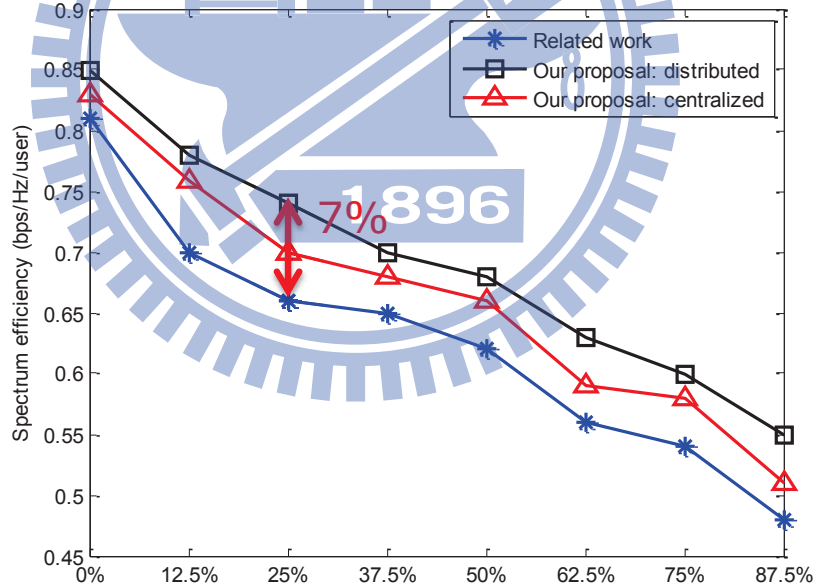


Figure 5.4: Comparison of our method and related work of macro-cell cell edge users, where the number of pico-cell is 12

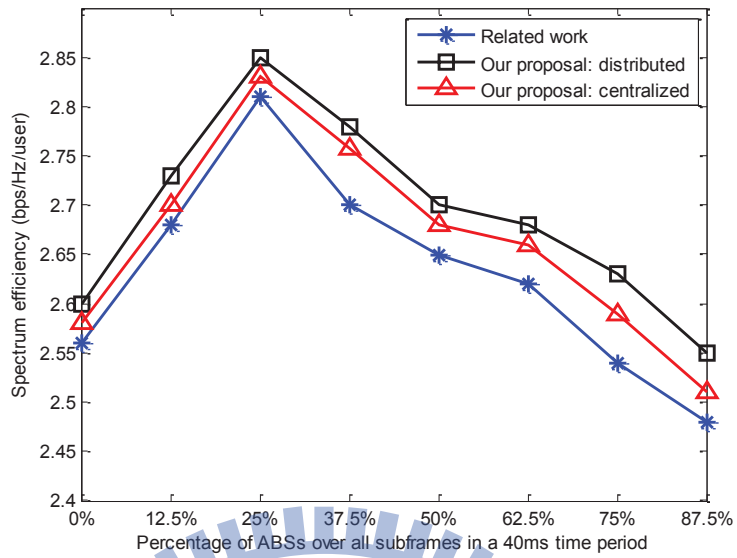


Figure 5.5: Comparison of mean throughput of our method and related work of cell edge users, where the number of pico-cell is 12

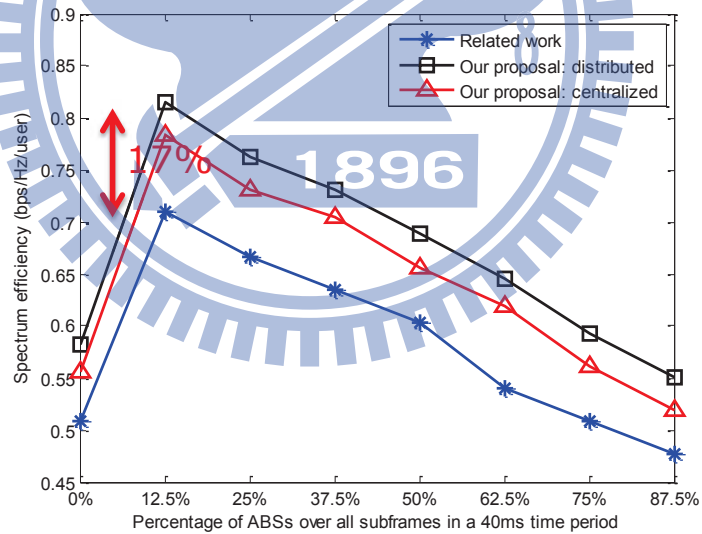


Figure 5.6: Comparison of our method and related work of cell edge users, where the number of pico-cell is 24

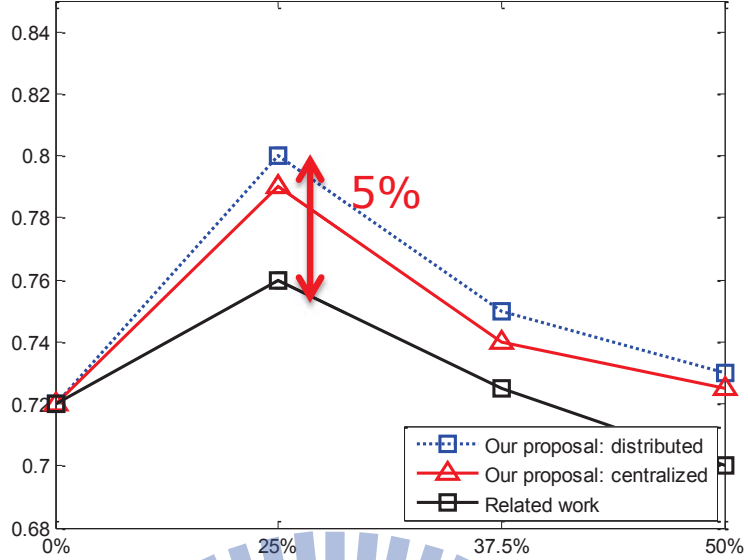


Figure 5.7: Fairness index of our method and related work of cell edge users, where the number of pico-cell is 12

### 5.3 Fairness of Our Method and Related Work

With Jain’s fairness index, our proposed method alleviates the fairness compared with [2]. Figure 5.7 shows the fairness comparisons of our methods, including distributed and centralized method, and related work. Our methods can mitigate the interference from macro-cell and alleviate the cell edge users throughput, allocate resource to the users with bad performance. From Figure 5.7, the fairness indexes are the same at 0% ABS percentage, because there is no ABS techniques adopted here. While the spectrum efficiency reaches the climax at 25% ABS percentage, which is around 0.8, and decline afterwards. Our methods can reach additional 5% fairness index compare to related work. This phenomenon corresponds to the results stated before at Figure 5.3, where the climax locates at 25% ABS percentage. Hence, we can conclude that our method can improve the fairness and spectrum efficiency of users.

## 5.4 Prediction of Throughput

In order to simplify algorithm computation, we predict the interference index data and throughput matrix at time period  $t-1$ , and also made a comparison with the total throughput at time period  $t$ . Figure 5.8 shows that throughput of prediction is lower than our real-time result by 5% error with 25% ABS percentage, but our prediction still performs better than related work by 5%. This figure also shows the same phenomenon with before, which reaches climax at 25%, 0.75 (bps/Hz/users) and declines afterwards with 12 pico-cells. It is because of the trade-off of pico-cell users and macro-cell users throughput gain, and reach climax at 25%.

Prediction of throughput are based on the definitions listed below:

$Z_t$  is the throughput matrix at time period  $t$ .

$K_t$  is the interference indication at time period  $t$ .

$Z_{t-1}$  is the throughput matrix at time period  $t-1$ .

$K_{t-1}$  is the interference indication at time period  $t-1$ .

$\frac{Z_t}{K_t}$  is the real time throughput at time period  $t$ .

$\frac{Z_{t-1}}{K_{t-1}}$  is the throughput of prediction from time period  $t-1$ .

## 5.5 Uplink Side Transmission

In uplink side transmission, we apply SC-FDMA, and SINR-based selection method for users to choose its serving base station. Interference-aware adaptive ABS distributed and centralized allocated methods are also taken into consideration.

Table ?? shows the parameters for uplink transmission in details. Figure 5.9 shows the performance that our centralized and distributed methods outperform with related work about 13%, which is the same results as downlink side. With 12 pico-

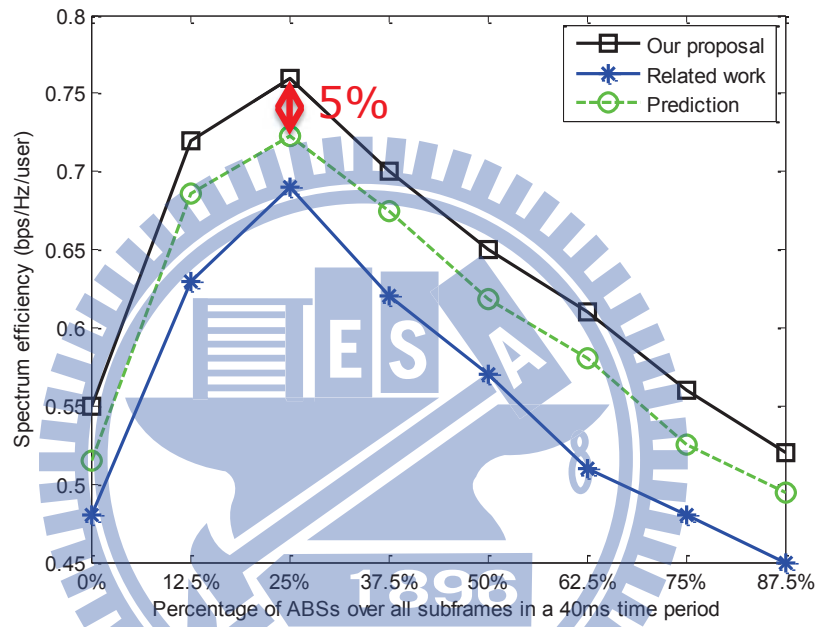


Figure 5.8: Comparison of throughput prediction and related work

Table 5.3: Simulation parameters of uplink transmission for macro-cell [1]

Parameter	Value
Link Direction	Uplink with SC-FDMA
Bandwidth	10 MHz
Macro-cell layout	19 Base Stations
Inter-site distance	500 meters
Penetration Loss	$128.1+37.6*\log_{10}(d)$ , d in km
User Tx Power	23 dBm
Noise Power Density	-174 dBm/Hz
Shadowing	8 dB
User speed	3 km/hr

cells, the spectrum efficiency reach 0.135 (bps/Hz/user) and 0.128 (bps/Hz/user) at 25% for centralized and distributed methods, and related work gets only 0.119 (bps/Hz/user). Spectrum efficiency here is comparatively small than downlink side, since the transmitting power of mobile users is small and the differences between OFDMA and SC-FDMA.

Hence, we can summarize that our adaptive ABS allocation methods can also enhance uplink side transmission throughput, where distributed allocation method can perform even better than centralized one.

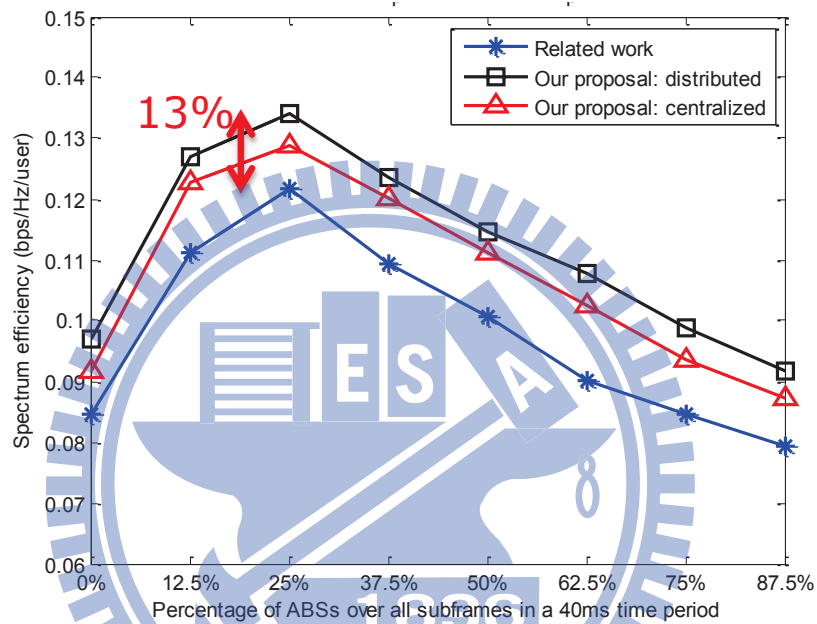


Figure 5.9: Comparison of our method and related work of cell edge users for uplink transmission, where the number of pico-cell is 12

# CHAPTER 6

## Conclusion

### 6.1 Conclusions

In this thesis, we developed two interference-aware adaptive ABS allocation methods in eICIC time domain, which are distributed and centralized methods for ABS times slots allocation. Different from the original method of fixed ABS patterns and ABS percentage, we determine a interference index to reallocate ABS subframes in order to maximize the total throughput of each time frame, and furthermore maximize the total throughput of macro-cell and pico-cells in each single cell. From numerical results in previous section, we could know that ABS can enhance throughput dramatically when macro-cells and pico-cells share the same frequency band. If ABS percentage has been faulty determined, spectrum efficiency will decrease. Hence, our proposed method is here to solve this problem. The results show that we could improve the throughput with lower ABS percentage and achieve higher throughput. Moreover, we could ensure that the throughput of macro-cell user without sacrificing too much throughput in order to compensate pico-cell's users. In the considered case, the throughput of pico-cells and macrocell are improved by at least 13% and 7% respectively, compared to the current fixed ratio ABS design approach.



## Bibliography

- [1] 3GPP, TR 36.814 (v9.0.0), “3rd generation partnership project: Technical specification group radio access network; evolved universal terrestrial radio access (E-UTRA); further advancements for e-UTRA physical layer aspects,” Mar. 2010.
- [2] K. Okino and C. Yamazaki, “Pico cell range expansion with interference mitigation toward LTE-Advanced heterogeneous networks,” *IEEE International Conference on Communications (ICC Workshops '11)*, 2011.
- [3] M. Vajapeyam, “Downlink FTP performance of heterogeneous networks for LTE-Advanced,” *IEEE International Conference on Communications (ICC Workshops '11)*, Jun. 2011.
- [4] K. Balachandran, “Cell selection with downlink resource partitioning in heterogeneous networks,” *IEEE International Conference on Communications (ICC Workshops '11)*, Jun. 2011.
- [5] R. Madan and T. Ji, “Cell association and interference coordination in heterogeneous LTE-A cellular networks,” *IEEE Journal on Selected Areas in Communications*, vol. 28, no. 9, pp. 1479–1489, Dec. 2010.
- [6] T. Hu and P. Godin, “Chapter 31: Additional features of LTE release 10,” in *LTE- The UMTS Long Term Evolution: From Theory to Practice*, 2011, pp. 701–714.
- [7] A. Damnjanovic and J. Montojo, “A survey on 3GPP heterogeneous networks,” *IEEE Wireless Communications Magazine*, pp. 10–21, Jun. 2011.
- [8] J. T. Aamod Khandekar, Naga Bhushan and V. Vanghi, “LTE advanced: Heterogeneous networks,” *European Wireless Conference (EW '10)*, Qualcomm Inc., vol. 18, Feb. 2010.
- [9] G. J. S. L. Stefan Parkvall, Erik Dahlman and L. Lindbom, “Heterogeneous network deployments in LTE,” Ericsson, Feb. 2011.
- [10] J. D. N. Volker Pauli and E. Seidel, “Heterogeneous LTE networks and inter-cell interference coordination,” Nomor Research, Dec. 2010.

- [11] 3GPP, R1-100061, “On technical aspects on heterogeneous networks,” Jan. 2010.
- [12] 3GPP, R1-101505, “Extending Rel-8/9 ICIC into Rel-10,” Feb. 2010.
- [13] 3GPP, R1-101504, “Enhanced interference management for co-channel support of HetNet deployments,” Feb. 2010.
- [14] 3GPP TSG RAN WG1, “Comparison of time-domain eICIC solutions,” Aug. 2010.
- [15] 3GPP, R1-103713, “Views on PDCCH interference mitigation for Het-Nets,” Jun. 2010.
- [16] A. Barbieri and F. Xue, “Coordinated downlink multi-point communications in heterogeneous cellular networks,” *Information Theory and Applications Workshop (ITA)*, 2012.
- [17] G. Li and H. Liu, “Downlink radio resource allocation for multi-cell OFDMA system,” *IEEE Transactions on Wireless Communications*, vol. 5, no. 12, pp. 3451–3459, Nov. 2006.
- [18] C. Koutsimanis and G. Fodor, “A dynamic resource allocation scheme for guaranteed bit rate services in OFDMA networks,” *IEEE International Conference on Communications (ICC Workshops '08)*, pp. 2524–2530, 2008.
- [19] A. Abrardo, “Centralized radio resource allocation for OFDMA cellular systems,” *IEEE International Conference on Communications (ICC '07)*, pp. 5738–5742, 2007.
- [20] S. Roth and D. Danev, “Subframe allocation for relay networks in the LTE-Advanced standard,” *IEEE 21st International Symposium on Personal Indoor and Mobile Radio Communications (PIMRC)*, 2010.
- [21] A. R. Gabor Fodor, C. Koutsimainis, “Intercell interference coordination in OFDMA networks and in the 3gpp long term evolution system,” *IEEE Wireless Communications Magazine*, vol. 4, no. 7, pp. 445–453, Aug. 2009.
- [22] V. Pauli and E. Seidel, “Inter-cell interference coordination for LTE-A,” Sep. 2011.
- [23] I. Gvenc and M.-R. Jeong, “Range expansion and inter-cell interference coordination (ICIC) for picocell networks,” *IEEE Vehicular Technology Conference (VTC Fall)*, pp. 1–6, Fall 2011.

# Vita

## **Wen-Pin Lai**

He was born in Taiwan, R. O. C. in 1988. He received his B.S. at the Department of Communication Engineering, National Chiao-Tung University in 2010. From July 2010 to August 2012, he worked his Master degree in the Mobile Communications and Cloud Computing Lab at the Institute of Communication Engineering at National Chiao-Tung University. His research interests are in the field of wireless communications.

